Cell Reports, Volume *42*

Supplemental information

Structural changes in the SARS-CoV-2 spike E406W mutant escaping a clinical monoclonal antibody cocktail

Amin Addetia, Young-Jun Park, Tyler Starr, Allison J. Greaney, Kaitlin R. Sprouse, John E. Bowen, Sasha W. Tiles, Wesley C. Van Voorhis, Jesse D. Bloom, Davide Corti, Alexandra C. Walls, and David Veesler

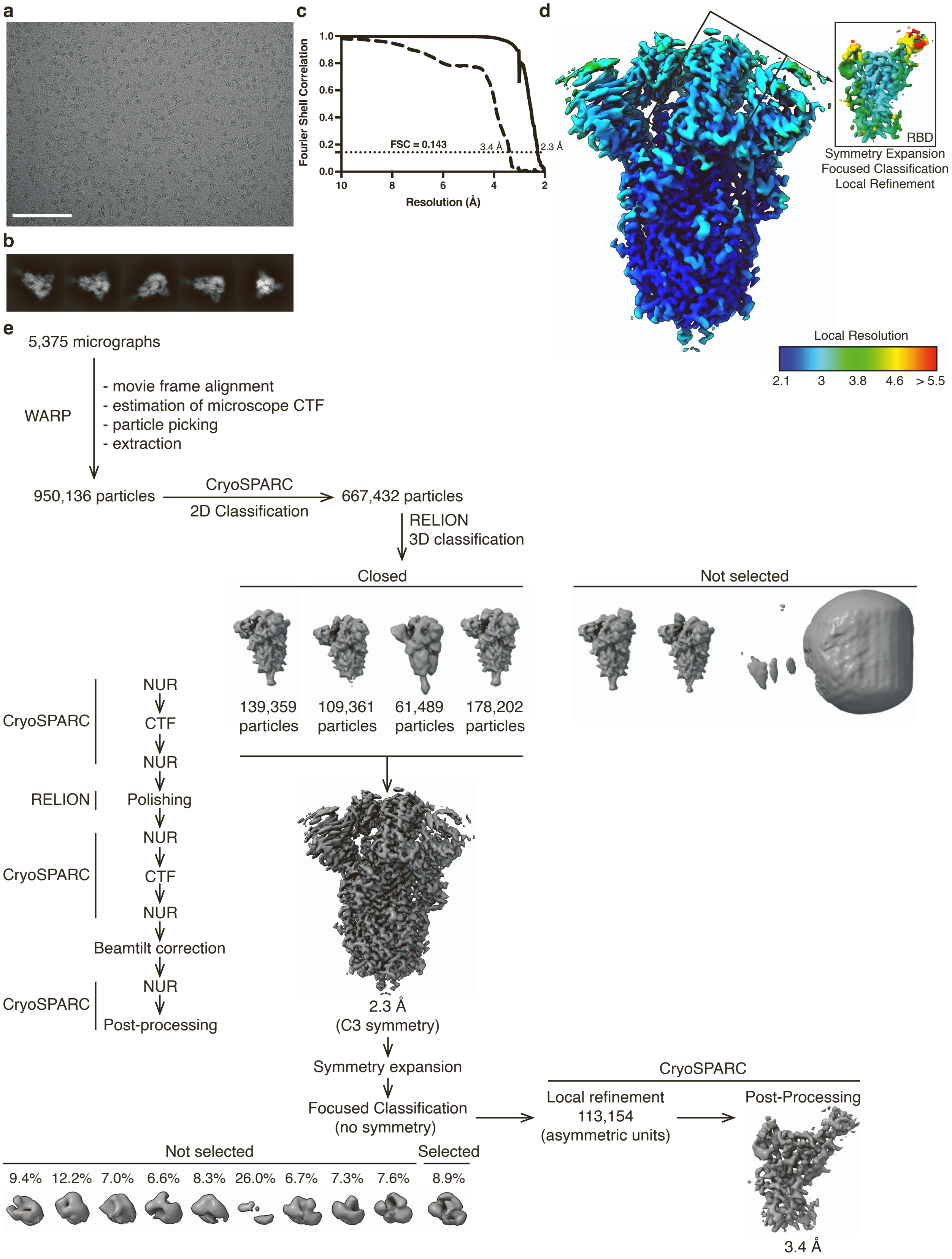
a
b
c
1.0
0.8
0.6
0.4
0.2
0.0
Fourier Shell Correlation
FSC = 0.143
3.4 Å
2.3 Å
10
8
6
4
2
Resolution (Å)
d
RBD
Symmetry Expansion
Focused Classification
Local Refinement
Local Resolution
2.1
3
3.8
4.6
> 5.5
e
5,375 micrographs
WARP
- movie frame alignment
- estimation of microscope CTF
- particle picking
- extraction
950,136 particles
CryoSPARC
2D Classification
667,432 particles
RELION
3D classification
Closed
Not selected
139,359 particles
109,361 particles
61,489 particles
178,202 particles
CryoSPARC
NUR
CTF
NUR
RELION
Polishing
NUR
CryoSPARC
CTF
NUR
Beamtilt correction
NUR
CryoSPARC
Post-processing
2.3 Å
(C3 symmetry)
Symmetry expansion
Focused Classification
(no symmetry)
CryoSPARC
Local refinement
113,154
(asymmetric units)
Post-Processing
3.4 Å
Not selected
Selected
9.4%
12.2%
7.0%
6.6%
8.3%
26.0%
6.7%
7.3%
7.6%
8.9%

Figure S1. cryo-EM processing and validation for the SARS-CoV-2 E406W spike dataset; related to Figure 1 and STAR Methods**. a-b,** Representative electron micrograph (a) and 2D class averages (b) obtained for the SARS-CoV-2 E406W spike ectodomain. Scale bar: 100 nm. (c) Gold-standard fourier shell correlation curves for the closed E406W S trimer (solid line) and locally refined E406W RBD (dashed line). **d,** Local resolution calculated using CryoSPARC for the E406W S ectodomain trimer (left, unsharpened map) and the locally refined RBD (right, sharpened map). **e,** cryo-EM processing workflow.

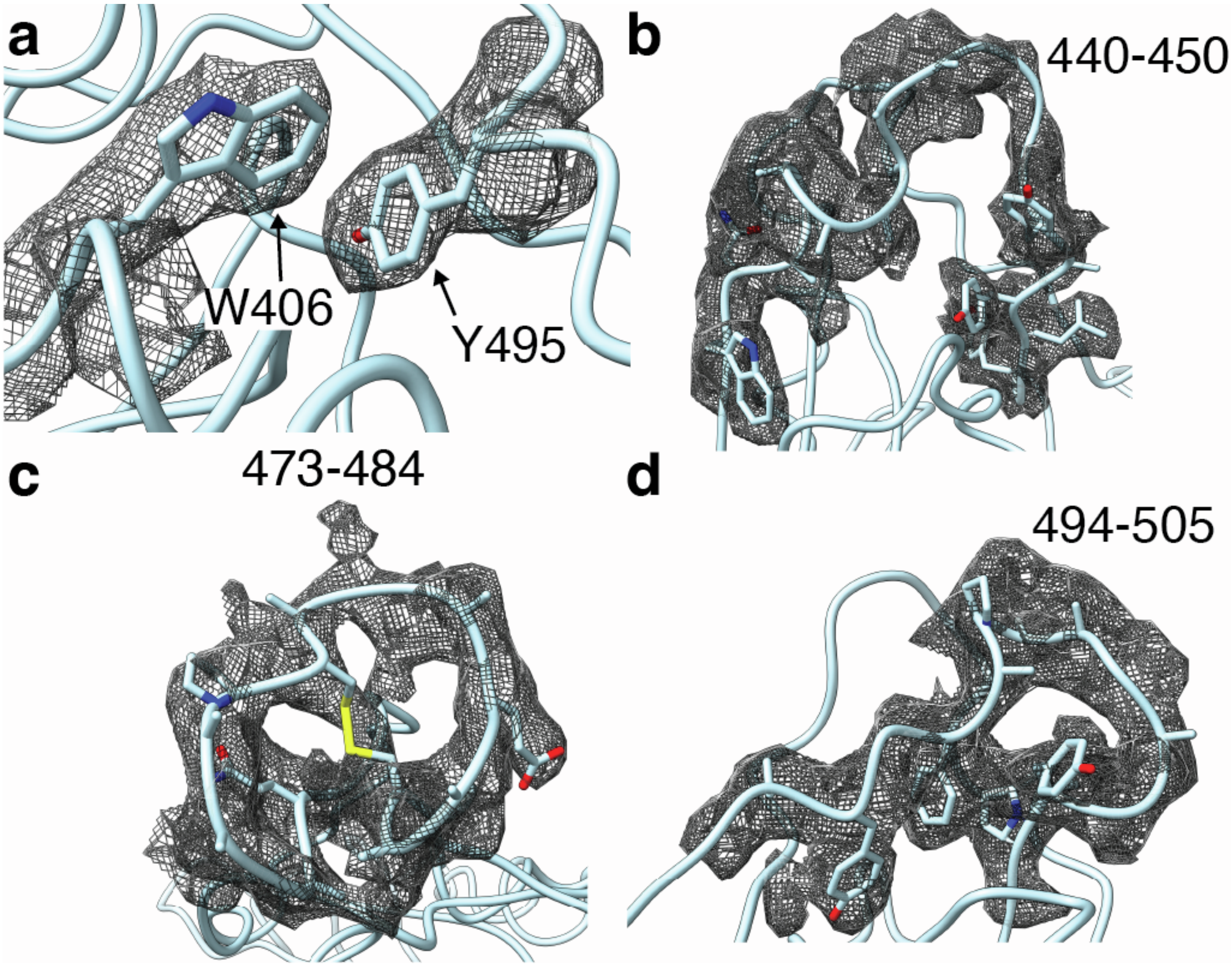

Figure S2. Support for the structural rearrangements in the W406 RBD with the locally refined cryo-EM map; related to Figure 1. Cryo-EM map, represented as a black mesh, obtained from local refinement of the RBD and the W406 RBD model compared to show the areas in which the W406 RBD diverges most significantly from the E406 RBD, including (**a**) the Y495 sidechain, (**b**) residues 440-450, (**c**) residues 473-484, and (**d**) residues 494-505.

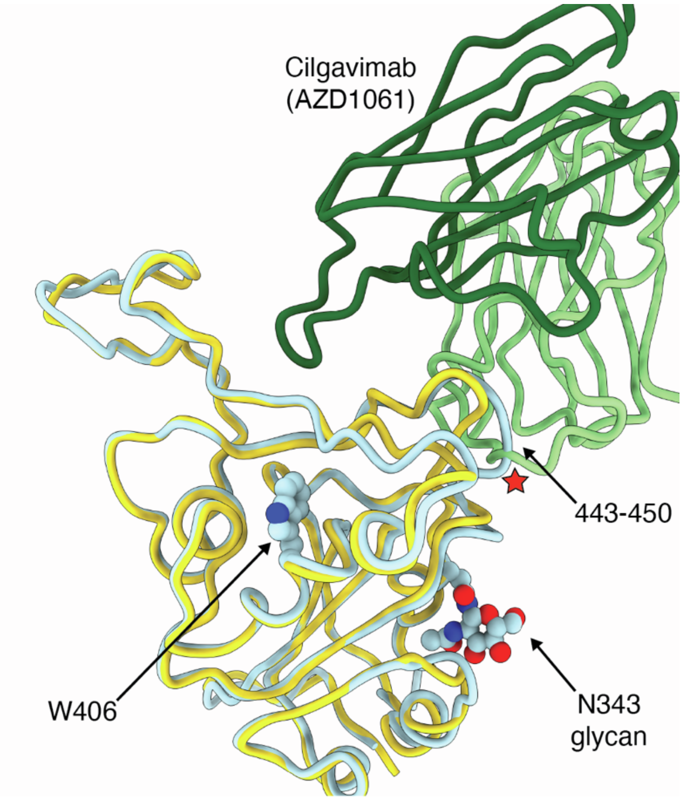

Figure S3. Repositioning of residues 443-450 in the W406 RBD interferes sterically with cilgavimab binding; related to Figure 1. Structural superimposition of the cilgavimab (AZD1061)-bound Wuhan-Hu-1 RBD (E406, gold, PBD 7L7E) and the W406 RBD (light blue). Key reorganized regions are labeled and the steric clash is indicated by a red star.

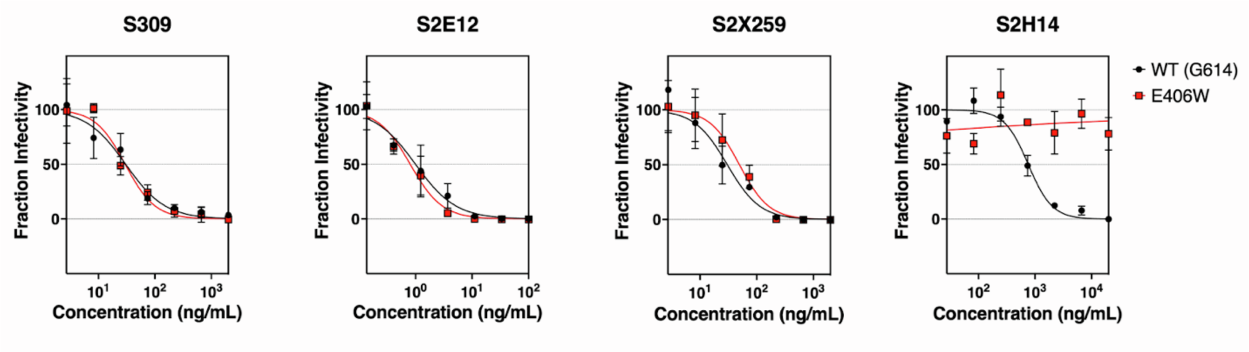

Figure S4; related to Table 1 and Figure 3. Neutralization curves for E406W/G614, shown in red, or wildtype (G164), shown in black, pseudotyped VSV using four monoclonal antibodies targeting the SARS-CoV-2 RBD. Neutralization assays were performed in triplicate and replicated twice with two batches of pseudovirus.

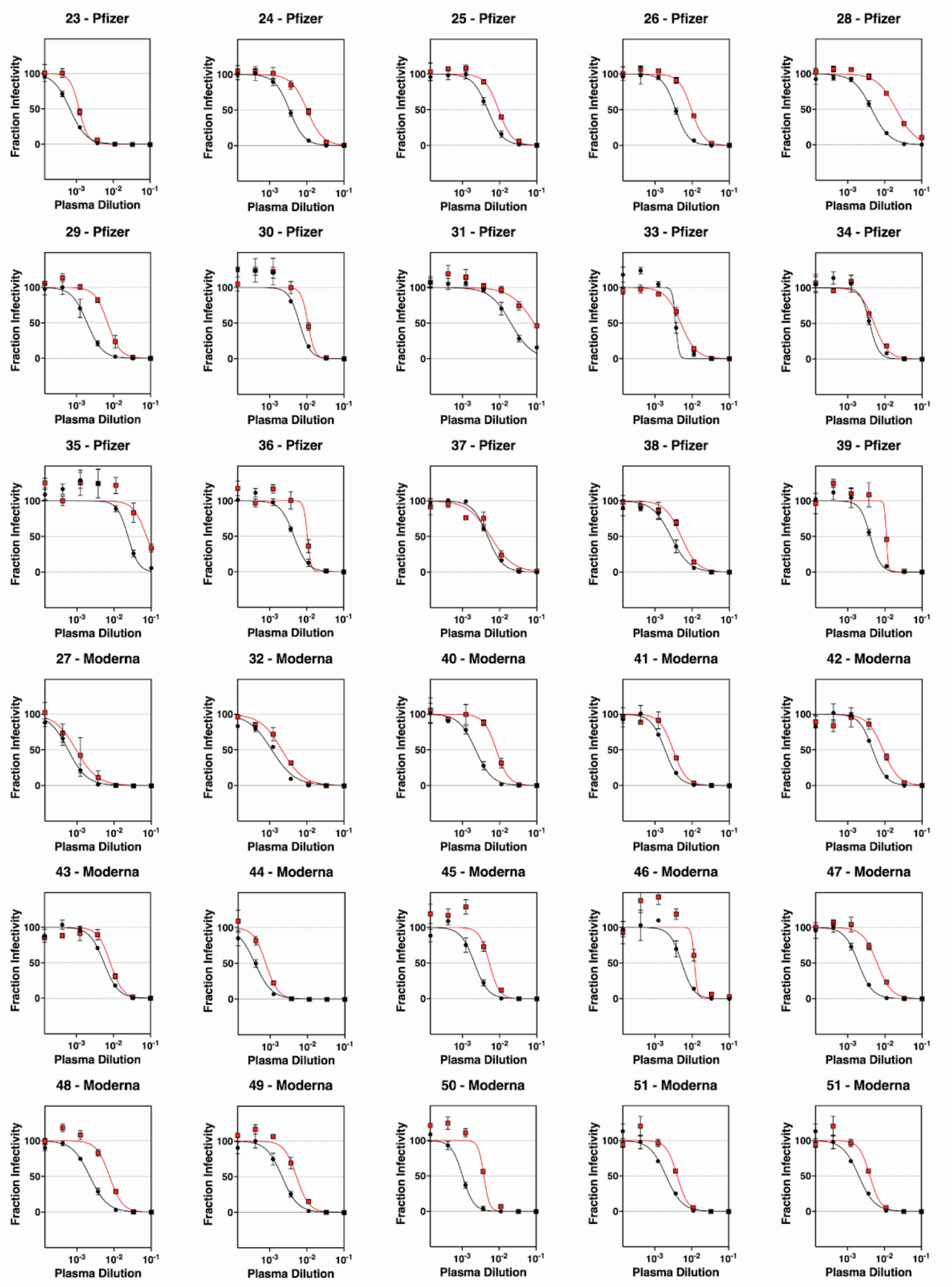

Figure S5; related to Figure 3. Neutralization curves against E406W/G614 S, shown in red, or wildtype (G614) S, shown in black, pseudotyped VSV for 30 sera samples collected from individuals vaccinated with either Pfizer BNT162b2 or Moderna mRNA-1273 COVID-19 vaccines. Neutralization assays were performed in triplicate and repeated at least twice with at least two distinct batches of pseudovirus.

Table S1. Cryo-EM data collection, refinement and validation statistics; related to Figure 1.

	SARS-CoV-2 S E406W Ectodomain (EMDB-26056) (PDB 7TPI)	SARS-CoV-2 S E406W RBD (local refinement) (EMDB-26058) (PDB 7TPK)
Data collection and processing		
Magnification	105,000	105,000
Voltage (kV)	300	300
Electron exposure ($e^-/Å^2$)	63	63
Defocus range (μm)	- 0.1 to -2.6	-0.1 to -2.6
Pixel size (Å)	0.843	0.843
Symmetry imposed	C3	C1
Initial particle images (no.)	950,136	1,281,585
Final particle images (no.)	427,195	113,154
Map resolution (Å)	2.3	3.4
FSC threshold	0.143	0.143
Map resolution range (Å)	2.2-8.9	2.8-9.1
Refinement		
Initial model used (PDB code)	7LXY	6M0J

Model resolution (Å)	2.3	3.4
FSC threshold	0.143	0.143
Map sharpening *B* factor (Å^2)	-71	-104
Model composition		
Non-hydrogen atoms	21,168	1,446
Protein residues	2,862	194
Ligands	54	1
B factors (Å^2)		
Protein	38.08	26.84
Ligand	21.98	23.50
R.m.s. deviations		
Bond lengths (Å)	0.012	0.012
Bond angles (°)	1.434	1.867
Validation		
MolProbity score	1.01	1.02
Clashscore	2.21	0.37
Poor rotamers (%)	0.49	0
Ramachandran plot		
Favored (%)	97.95	94.27
Allowed (%)	2.05	5.21
Disallowed (%)	0	0.52

Table S2. Binding kinetics of the RBD to human ACE2 as measured by biolayer interferometry. Values are presented as mean ± standard error; related to Figure 2.

	K_D (nM)	**k_{on} ($M^{-1}s^{-1}$)**	**k_{off} (s^{-1})**
WT	93.9 ± 3.3	1.4×10^{5}	1.2×10^{-2}
Alpha	10.9 ± 0.9	2.3×10^{5}	2.5×10^{-3}
E406W	1,335 ± 195	7.6×10^{4}	1.0×10^{-1}

Table S3. Demographic information for vaccine-elicited sera donors; related to Figure 3.

Study ID	Age	Vaccine Type	Days after second vaccination	Sex	Race	Ethnicity
23	60	Pfizer	11	M	White	Not Hispanic or Latino
24	65	Pfizer	10	M	White	Not Hispanic or Latino
25	55	Pfizer	18	M	White	Not Hispanic or Latino
26	42	Pfizer	9	F	White	Not Hispanic or Latino
27	66	Moderna	8	F	White	Not Hispanic or Latino
28	63	Pfizer	10	M	White	Not Hispanic or Latino
29	27	Pfizer	8	F	White	Not Hispanic or Latino
30	38	Pfizer	8	F	Asian	Not Hispanic or Latino
31	37	Pfizer	21	F	Black	Not Hispanic or Latino
32	36	Moderna	7	M	White	Not Hispanic or Latino
33	62	Pfizer	15	M	Pacific Islander	Not Hispanic or Latino
34	54	Pfizer	14	F	White	Not Hispanic or Latino
35	60	Pfizer	14	F	White	Not Hispanic or Latino
36	32	Pfizer	13	F	White	Not Hispanic or Latino
37	52	Pfizer	11	M	White	Not Hispanic or Latino
38	61	Pfizer	9	M	White	Not Hispanic or Latino
39	32	Pfizer	22	F	White	Not Hispanic or Latino
40	40	Moderna	20	M	White	Not Hispanic or Latino
41	64	Moderna	16	M	White	Not Hispanic or Latino
42	34	Moderna	23	F	Asian	Not Hispanic or Latino

43	22	Moderna	20	F	White	Not Hispanic or Latino
44	24	Moderna	18	F	White	Not Hispanic or Latino
45	35	Moderna	20	M	White	Not Hispanic or Latino
46	40	Moderna	24	M	White	Not Hispanic or Latino
47	55	Moderna	20	M	White	Not Hispanic or Latino
48	25	Moderna	22	M	White and Asian	Not Hispanic or Latino
49	26	Moderna	18	F	White	Not Hispanic or Latino
50	36	Moderna	27	F	Asian	Not Hispanic or Latino
51	53	Moderna	20	F	White	Not Hispanic or Latino
52	47	Moderna	21	M	White	Not Hispanic or Latino